DEVELOPMENT AND TESTS OF A HYDRAULIC SWIVEL DRIVE WITH HYDROSTATIC BEARINGS

Lutz Müller[1]*, Jürgen Weber[1], Jannis Rühe[2], Frank Biller[2]

[1]*Institute of Mechatronic Engineering, Technische Universität Dresden, Helmholtzstrasse 7a, 01069 Dresden*
[2] *Homrich Maschinenbau GmbH, Nieland 3, 23611 Bad Schwartau*

* Corresponding author: Tel.: +49 351 463-33705; E-mail address: lutz.mueller@tu-dresden.de

ABSTRACT

Hydraulic swivel drives from SÜDHYDRAULIK by Homrich Maschinenbau GmbH are widely used for different applications. Especially for oscillating movements with high frequencies and for integration of functions as thrust bearings, the axial load bearing capacity of the drives had to be improved. To achieve this goal, a hydrostatic thrust bearing was designed for the high load series swivel drive SP 15 D. In a first attempt the design was focused on achieving the highest possible load at operating pressure of the swivel drive with an acceptable leakage flow. The analytic calculations were executed according to common literature, but supplemented with FEM simulations and test data to consider elastic deformations. The test of the prototype showed a good agreement with the calculation results.

Keywords: Hydrostatic Axial and Radial Bearing, Swivel Drives

1. INTRODUCTION

Hydraulic swivel drives are widely used for different applications ranging from the movement of simple cargo doors once in some weeks to highly complex testing machines. Especially for testing setups and testing machines the rotational movement has to change the direction with very high frequency of sometimes more than 10 Hz applying also high load moments to test materials or components.

A further challenge is the rotation angle. For the high-speed series it is a maximum of 110 degrees but particularly at testing machines the rotation angle can be very small. Often it is not possible to use separate bearings to compensate axial and radial forces, which leads to additionally high loads on the bearing structure of the swivel drive. Thus, not only a few practical operating conditions of swivel drives can be destructive for rolling bearings, which are typically used in these applications.

To extend the operating limits of the swivel drives resulting from conventional rolling bearings, hydrostatic bearings were developed to carry the axial loads. The bearing configuration and geometry was designed according to commonly available literature, mostly summarized by Weck and Brecher [1], whereas this summary does mostly rely on Optitz [2]. But in the real application the deformations of the bearing geometry due to pressure and loads have to be calculated with FEM to ensure a maximum load bearing with small oil through-flow.

For verification of all calculations a comprehensive test program was passed, that ensured the operating parameters of the newly developed bearing system.

2. BEARING DESIGN

2.1. Design Considerations and Calculations

The swivel drive SP15D has very high torque and can withstand also high radial loads. Therefore it is equipped with the rolling bearings for a high radial load capacity. But the axial loads, such a swivel drive could handle, were limited due to a lubrication concept with a restricted ability for self-centring of the rotary piston.

To improve the axial load capacity, a hydrostatic thrust bearing was integrated with the aims not to change the existing rolling bearing setup, not to change dimensions and manufacturing processes of the existing case design and obtain the highest axial load capacity which is possible. A further restriction was, to achieve a leakage flow of the hydrostatic thrust bearing which should be not more than the one, which was required by the well approved lubrication concept.

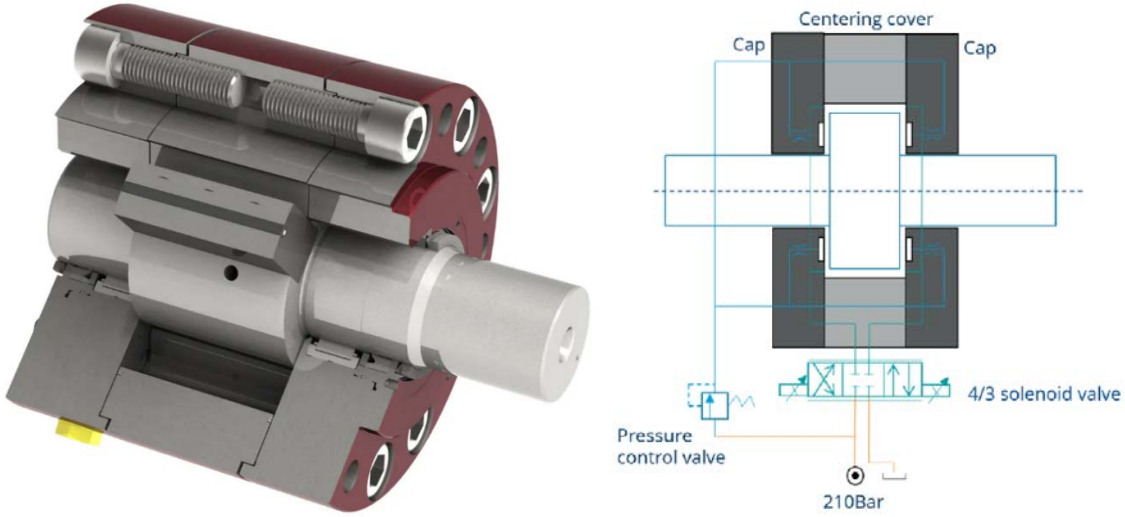

Figure 1: Swivel drive SP 15 D and typical hydraulic layout of the thrust bearing

$$d_m = \frac{d_o + d_i}{2} \quad (1)$$

$$b = 2\pi d_m \quad (2)$$

$$A_{eff} = \pi d_m (B_B - l) \quad (3)$$

$$Q = \frac{p b h^3}{12 \eta l} \quad (4)$$

$$R = \frac{p}{Q_L} = R_P + R_K = \frac{p - p_P}{Q_L} + \frac{p_P}{Q_L} \quad (5)$$

$$R = \frac{12\eta l}{b h^3} + \frac{128 \eta l_k}{\pi d_K^4} \quad (6)$$

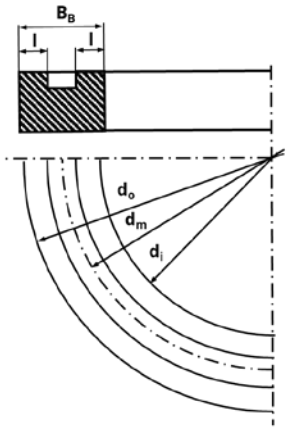

$$p_P = p \cdot \frac{R_P}{R_K + R_P} \quad (7)$$

$$R_P = \frac{p_P}{Q} \quad (8)$$

$$R_P = \frac{12\eta l}{b h^3} \quad (9)$$

$$h_Q = \sqrt[3]{\frac{12\eta l Q}{p b}} \quad (10)$$

$$F_{ax} = p_P \cdot A_{eff} \quad (11)$$

$$P_{bear} = p \cdot 2 Q_L \quad (12)$$

Figure 2: Geometry of the bearing grove and design calculations (according to [1] and [2])

Initially the deformation of the shaft was estimated to be much less than the usual manufacturing tolerances of the internal gaps of the swivel drive. This means, the final design of the axial bearing groves could be established as one continuous grove with constant width B_B with sealing edges of equal width l.

For the design of the bearings pocket pressures regulating device at first different concepts were analysed including a membrane type valve. But, since the final design of the bearing should be easy to set up and to maintain but also able to deal with all typical applications of the swivel drives, for instance also only low levels of fluid cleanliness, the concept of capillary restrictors was preferred.
According to [1] and [2] the design calculations are given as shown in ***Figure 2***. These show only one difficulty.

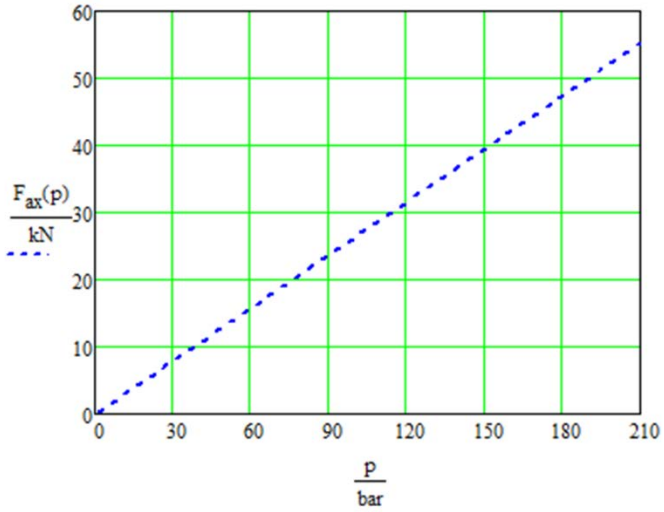

Figure 3: maximum axial load of an ideal hydrostatic bearing which could be realized in a SP15D swivel drive

For optimum work performance of the bearing the resistance ratio $\xi = \frac{R_K}{R_{P0}} \approx 1$ should be nearly 1 [1]. To achieve this, at first, the manufacturing tolerances were measured and a predesign was calculated but the confidence in these data was questionable because the swivel drives structure was suspected to show certain elastic deformation under the high pressures which are normally applied to the bearings and the rotary piston.
Ideally with no deformation and therefore constant capillary and bearing resistances one can calculate the maximum load the bearing would resist by equations (1) to (11) resulting in a maximum axial load F_{ax} depending on the supply pressure p which can be seen in ***Figure 3***.
But in reality the swivel drive will show a distinct pressure dependent deformation, which could be calculated by a FEM simulation with limited effort. But the influences of manufacturing and assembly processes on the practically achievable bearing gap heights were neither possible to be calculated, nor be possible to be measured at the assembled operational swivel drive on another than a fluid mechanic way.
Thus, an experiment was setup to measure the supply pressure dependent volume flow and the resulting symmetrical one-sided bearing gap height.

2.2. Measurement Setup and Results

A test stand according to **Figure 4** (left side) was set up to measure the supply pressure dependent volume flow through the axial hydrostatic bearing. The real test stand can be seen in ***Figure 6***. Since no capillaries were installed yet, nearly the complete pressure drop results from the bearing geometry.

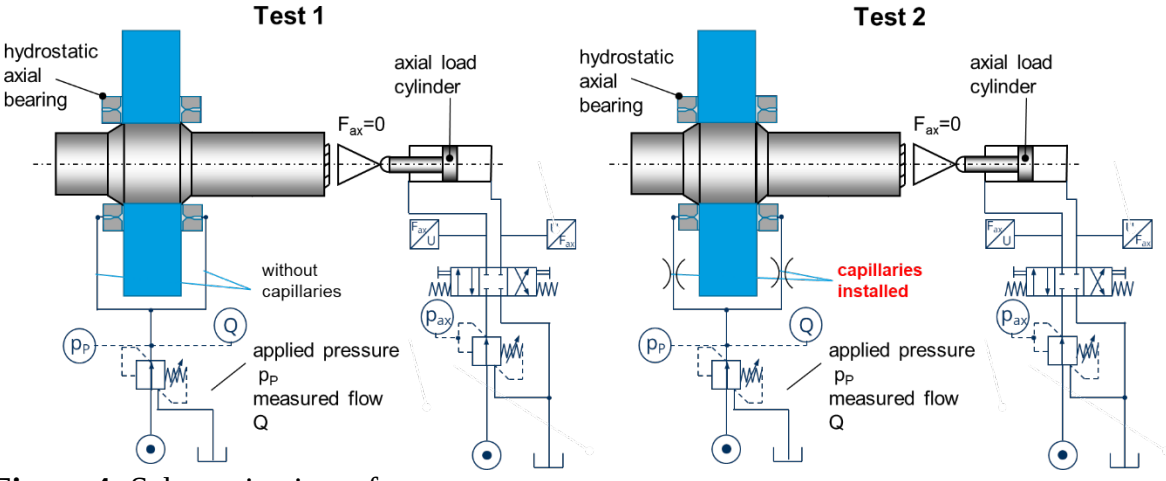

Figure 4: Schematic view of test setups

Because the resistance of the bearing pocket can be calculated with $R_P = \frac{p_P}{Q} = \frac{12\eta l}{bh^3}$, the integral gap height of the bearing can be calculated from the known dynamic viscosity (oil type and measured temperature), the bearings sealing strip width l and B according to the bearings mean circumference b. The mean gap height, which is resulting from these measured data is very precisely evaluated with the following equation. $h_Q = \sqrt[3]{\frac{12\eta l}{Qpb}}$

A big advantage of this procedure is that the behavior of the gap height is obtained for the complete functionally assembled swivel drive, only lacking the capillaries.

As can be seen in ***Figure 5*** left, the flow rate without capillaries is not linear but follows very precisely a quadratic equation. One could suspect non laminar flow behavior but a check of Reynolds-numbers lead to the assumption that this behavior is due to elastic deformation of the swivel drives structure due to the internal pressure at the operational conditions of the bearing. To check this thesis a FEM-model of the complete swivel drive was set up. Simulations were executed for two pocket pressures of 105 bar and 210 bar. The results are presented in the next section.

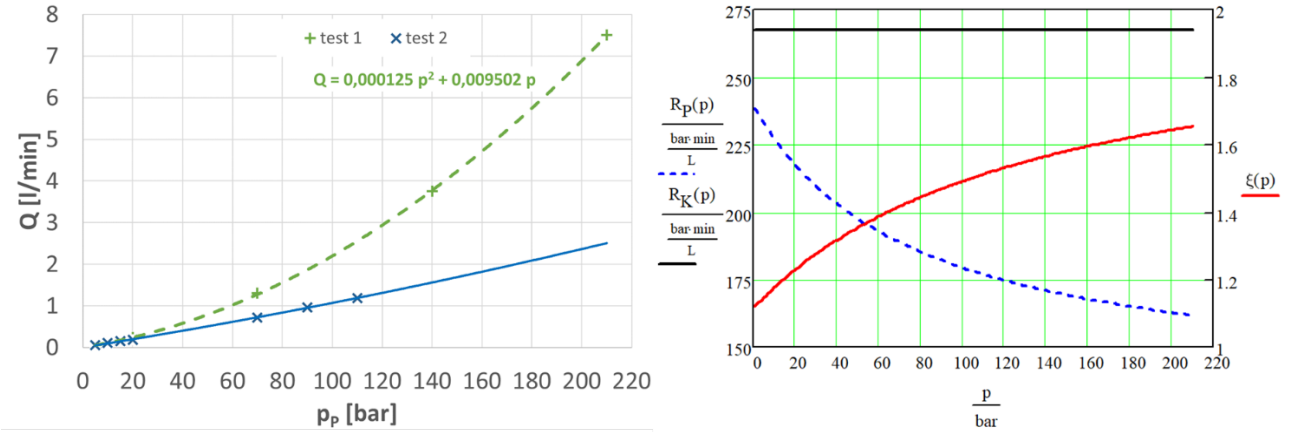

Figure 5: Left: measured flow characteristic for test 1 and 2 accord to **Figure 4** and **Figure 6** and right: the calculated resistances of the bearing pocket (R_P), used capillary (R_K) and resulting ξ

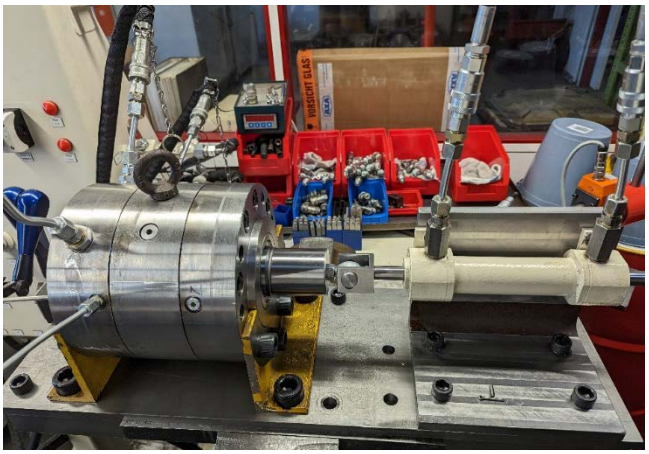

Figure 6: Swivel drive SP 15 D at the test stand for test 1 and 2

But with test 1 already done, it is possible to calculate the supply pressure depending bearings pocket resistance $R_P(p)$ according to equation (9) in ***Figure 2*** as can be seen in ***Figure 5*** on the right side. From the starting value at approximately 1 bar where $R_P(p) = 238{,}5$ bar min / L, one can also determine the capillary design. In the current example the capillary resistance was set to be $\xi = 1{,}12$.

For test 2 these capillaries were installed in the swivel drives and the through flow test was repeated. The result this test can be seen as blue crosses and blue line in ***Figure 5***. It shows a nearly perfect linear behavior. But since the thesis was not yet proven if the deformation of the swivel drive by internal bearing and load pressures really is the root cause for the pressure dependent gap height, an FEM simulation of the deformation of the structure by internal pressures was done and presented in the next chapter.

2.3. Refining the Design Calculations with FEM

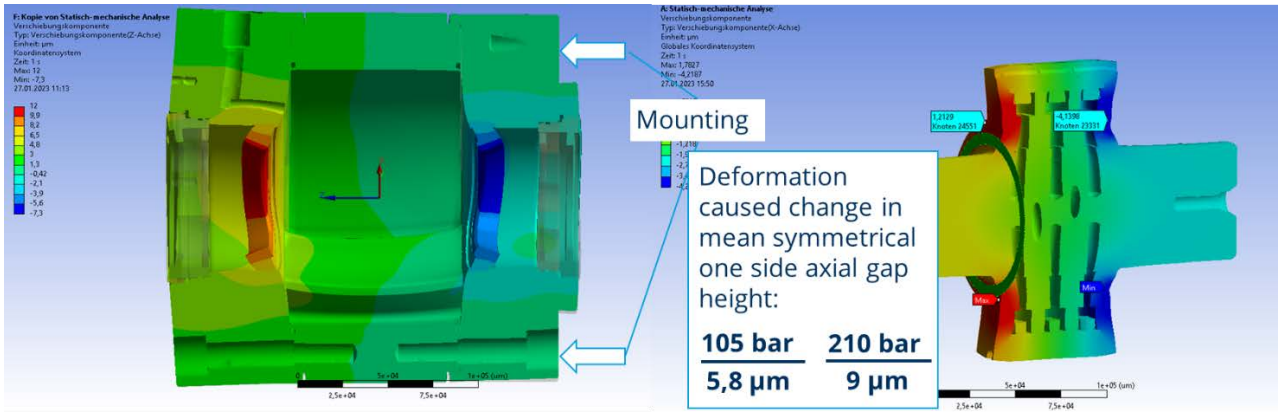

Figure 7: Simulation of the complete deformation of the swivel drive at two pocket pressures

The deformations of the swivel drive under service pressure and pocket pressures of 105 bar and 210 bar are to be seen in **Figure 7**. A typical one sided, symmetrical bearing gap height of 16,5 µm without any loads lead to a deformation which is not straight linear any more up to 210 bar pocket pressure. The value of initially 16,5 µm gap height as well as the calculated pressure dependent gap height (shown as green + in ***Figure 8***) according to equation (10) in ***Figure 2***.

The mean gap height from the FEM-calculated deformation and the approximation formula resulting from these simulations are shown in ***Figure 8***. It is clearly to be seen that the bearing gap height (o FEM) and the calculated bearing gap height from measurement data (+ measurement) show the similar behavior depending on the supply and internal pressure, respectively. That means the deformation of the swivel drives shaft and housing around the hydrostatic bearing is clearly the root cause for the gap behavior.

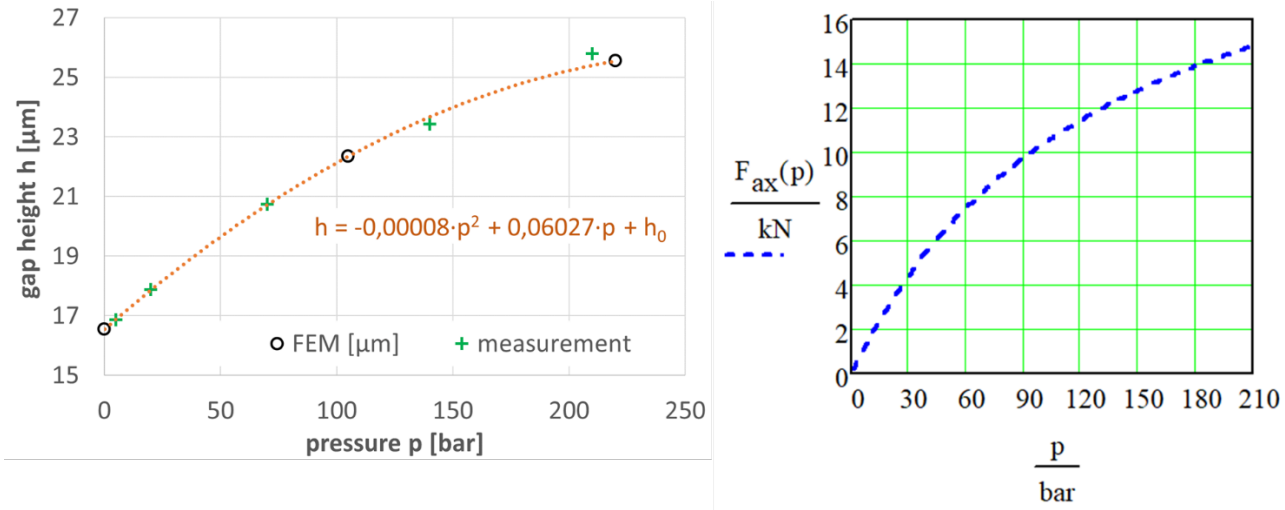

Figure 8: left: Comparison of measured and simulated symmetrical one side bearing gap height right: Calculated maximum axial bearing load

With these data available it is possible to calculate the maximum axial forces the hydrostatic bearing is able to withstand. Therefore the axial force $F_{ax}(p)$ was calculated by using formula (10) whereas p_T was calculated by (7) and A_{eff} results from the geometry of the bearing (3).
The results are given for different bearing supply pressures in the diagram on the right side of **Figure 8**. With a maximum supply pressure of 210 bar a maximum axial force of 15 kN can be

compensated. Since the pressure rating of the swivel drive is given by 300 bar, this value could be further extended to 16,75 kN.

From the equations (5) and (6) given in **Figure 2** also the expected leakage flow of one ($Q_L(p)$) and both two bearing pockets ($2 \cdot Q_L(p)$) can be calculated by the approximation function which was derived from the FEM simulation results shown on the left side of ***Figure 8***. Comparison between the graphs of volume flow of the complete bearing both in ***Figure 9*** and in the left diagram in ***Figure 5*** shows a very good agreement, which is resulting from the very good agreement between FEM simulated bearing gap deformation and measurement of that one shown on the left side of **Figure 8**. To verify the design calculations, which are already assisted by test data and FEM simulations, a further test run was executed and will be discussed in the next chapter.

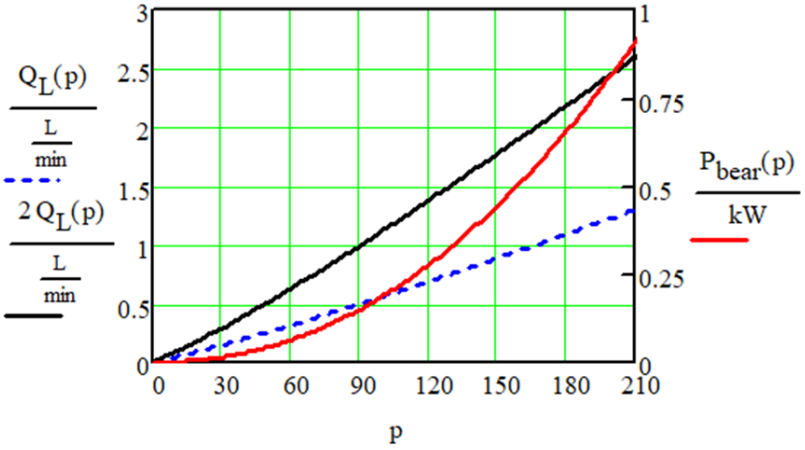

Figure 9: Leakage flow of one (Q_L) and both two bearing pockets ($2 \cdot Q_L$) calculated from FEM deformation and test data

3. EXPERIMENTAL VERIFICATION OF THE DESIGN

For the verification of the design the swivel drive SP15D was set up on the test bench where axial loads could be applied in both directions as can be seen in ***Figure 10*** and ***Figure 11***.

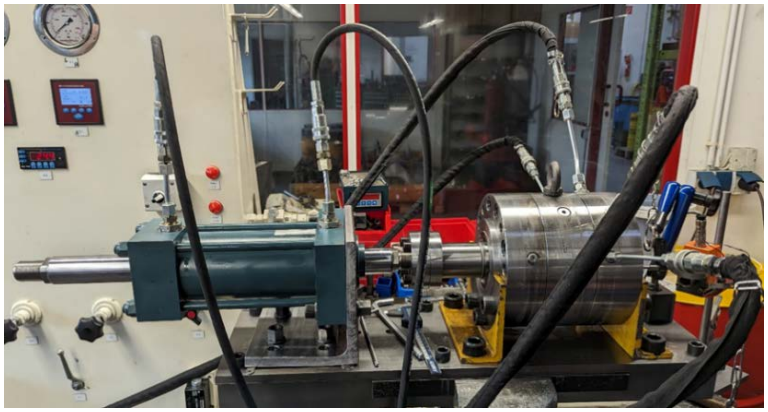

Figure 10: Swivel drive SP 15 D at the test stand for test 3 and 4

In test case 3 and 4 the startup pressure for the swivel drives rotary piston was measured for different axial loads which were applied using a linear cylinder. With this setup it is possible to obtain the axial load limit of the designed thrust bearing because the start-up pressure will significantly increase as soon as mixed or even contact friction will appear when the applied axial force exceeds the load force limit of the hydrostatic bearing. For the test cases 3 and 4 the bearing supply pressure was constantly at 120 bar. For this pressure, according to right diagram in **Figure 8**, one would expect an axial load force of 11,4 kN which could be sustained by the hydrostatic bearing.

The results of these measurements can be seen in **Figure 12**.

At axial load forces up to 12 kN, no increase of the start-up-pressure can be recognized. But further increase of the load lead also to an increase of the start-up-pressure. These data confirm the bearing design to be correct and verify the axial load limit of the bearing according to the right diagram in **Figure 8** too.

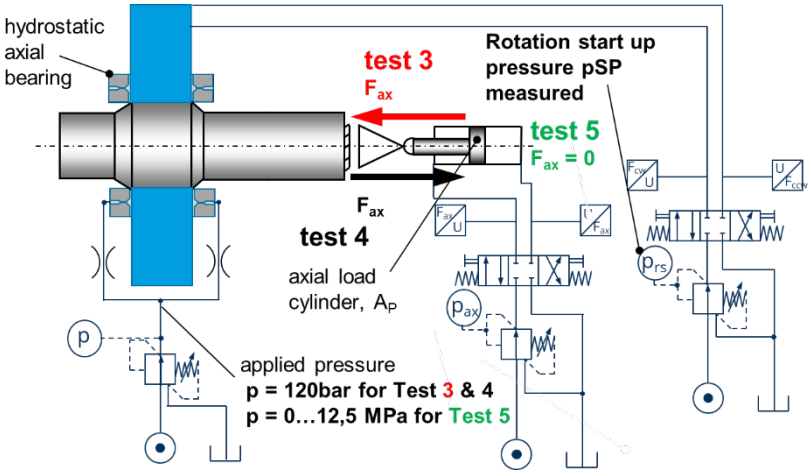

Figure 11: Schematic of the executed Tests 3 and 4

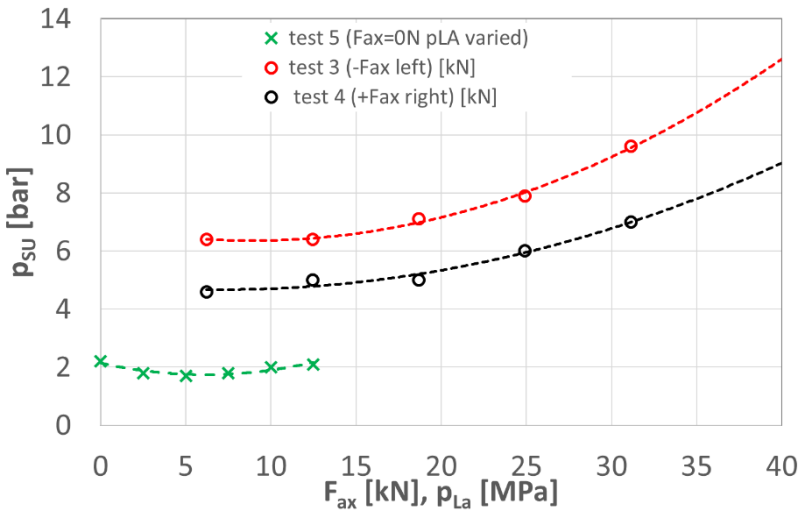

Figure 12: Measurement results from Tests 3 and 4 with a bearing supply pressure of 120 bar

For comparison, the start-up-pressure for test 5 is given. This is essential also for verifying a slight draw back of the test stand. In this test case there was no axial load force applied but the pressure of the hydrostatic bearing was varied. One can see a significantly lower start-up-pressure and also a difference in start-up-pressures between test 3 and 4 which lead to the assumption that the connection between the linear cylinder and the swivel drive is too ridged and the internal friction of the linear cylinders sealing system leads to the high start-up-pressures.
These could be either reduced by calibrated measurements or prevented by a more sophisticated bearing concept. Unfortunately, before the writing of this paper this was not possible to achieve but will be done afterwards to achieve a further development.

4. SUMMARY AND OUTLOOK

In this paper a new hybrid bearing concept for swivel drives was developed, using and verifying analytical design calculations for the hydrostatic axial bearing design whereas the radial bearings were well approved rolling bearings. Because the hydrostatic thrust bearings had to be integrated in the already well approved and reliable bearing concept, the remaining design space lead to limits which had been evaluated and improved by FEM simulations. With these and by test data, the design calculation of the load bearing capability and the required power consumption of the feed flow for the hydrostatic bearings were verified.
Simultaneously to the measurements, the axial bearing was implemented into a swivel drive of an industrial test stand application with over half a year of good experiences.

The design concept presented here was further developed to a not only axial but full hydrostatic axial and radial bearing concept of a new high speed swivel drive HSR14 which is of the same size as the SP15D. This one went already through the design process and is currently set up on a test stand for evaluation.

Supported by:

Federal Ministry
for Economic Affairs
and Climate Action

on the basis of a decision
by the German Bundestag

The presented research activities are part of the project "HYDROTACT – Hydrostatic Bearings for Svivel Drives" (Ref. No. **KK5023209RF1**), which was funded by the German Federal Ministry for Economic Affairs and Climate Action within the ZIM programme.

NOMENCLATURE

A_{eff}	mean effective load bearing area	mm²
b	mean bearing circumference	mm
B_B	width of the hydrostatic bearing	mm
d_i	inner bearing diameter	mm
dK	capillary diameter	mm
d_m	mean bearing diameter	mm
d_o	outer bearing diameter	mm
Fax	axial force	kN
h	mean bearing gap height	µm
h_Q	mean bearing gap height calculated from measurement data	µm
l	sealing edge width of the bearing	mm
l_K	capillary length	mm
p	supply pressure	bar
p_P	bearing pocket pressure	bar
P_{bear}	power required for bearing operation	kW
Q	volume flow	l min^{-1}
Q_L	one sided bearing pocket volume flow	l min^{-1}
R	resistance	bar min l^{-1}
R_K	capillary resistance	bar min l^{-1}
R_P	bearing pocket resistance	bar min l^{-1}
η	dynamic viscosity	kg $(m\ s)^{-1}$

REFERENCES

[1] Weck, M., Brecher, C. (2006) "Werkzeugmaschinen – Konstruktion und Berechnung", 8th edition, ISBN 3-540-22502-1, Springer Berlin Heidelberg New York

[2] Opitz, H. (1969) "Aufbau und Auslegugn Hydrostatischer Lager und Führungen und Konstruktive Gesichtspunkte bei der Gestaltung von Spindellagerungen mit Wälzlagern", Bericht über VDW-Konstrukteur-Arbeitstagung an der RWTH Aachen, Februar 1969